ARTICLE

Celastrol suppresses the growth of vestibular schwannoma in mice by promoting the degradation of β-catenin

Na Hui Kim[1], Minji Kwon[1], Jiwoo Jung[1], Hyo Byeong Chae[2], Jiwoo Lee[2], Yeo-Jun Yoon[3], In Seok Moon[3], Ho K. Lee[4], Wan Namkung[4], Konstantina M. Stankovic[5], Se A. Lee[6], Jong Dae Lee[6] and Sin-Aye Park[1,2]

Vestibular schwannoma (VS), one of characteristic tumors of neurofibromatosis type 2 (NF2), is an intracranial tumor that arises from Schwann cells of the vestibular nerve. VS results in hearing loss, tinnitus, dizziness, and even death, but there are currently no FDA-approved drugs for treatment. In this study, we established a high-throughput screening to discover effective compounds that could inhibit the viability of VS cells. Among 1019 natural products from the Korea Chemical Bank screened, we found that celastrol, a pentacyclic triterpene derived from a *Tripterygium Wilfordi* plant, exerted potent inhibitory effect on the viability of VS cells with an IC_{50} value of 0.5 μM. Celastrol (0.5, 1 μM) dose-dependently inhibited the proliferation of primary VS cells derived from VS patients. Celastrol also inhibited the growth, and induced apoptosis of two other VS cell lines (HEI-193 and SC4). Aberrant activation of Wnt/β-catenin signaling has been found in VS isolated from clinically defined NF2 patients. In HEI-193 and SC4 cells, we demonstrated that celastrol (0.1, 0.5 μM) dose-dependently inhibited TOPFlash reporter activity and protein expression of β-catenin, but not mRNA level of β-catenin. Furthermore, celastrol accelerated the degradation of β-catenin by promoting the formation of the β-catenin destruction complex. In nude mice bearing VS cell line SC4 allografts, administration of celastrol (1.25 mg·kg^{-1}·d^{-1}, i.p. once every 3 days for 2 weeks) significantly suppressed the tumor growth without showing toxicity. Collectively, this study demonstrates that celastrol can inhibit Wnt/β-catenin signaling by promoting the degradation of β-catenin, consequently inhibiting the growth of VS.

Keywords: celastrol; natural products; tumor growth; vestibular schwannoma; β-catenin degradation; Wnt/β-catenin

INTRODUCTION

Vestibular schwannoma (VS) is a non-malignant tumor that originates from Schwann cells of the vestibular nerve. It can occur unilaterally or bilaterally. VS is a typical tumor characteristic of neurofibromatosis type 2 (NF2), an inherited disorder caused by loss of the *NF2* gene encoding the tumor suppressor protein Merlin [1, 2]. VS not only causes hearing loss, tinnitus, and dizziness, but also causes facial paralysis, other cranial neuropathies, and even death from compression of the brainstem when the tumor grows [3]. Current treatment options for VS include microsurgery and stereotactic radiotherapy. However, these treatments carry significant risks, including irreversible ipsilateral hearing loss. Therefore, observation is the most common choice for most patients with VS tumors [4, 5]. Currently there are no approved pharmacological treatments for VS.

Wnt/β-catenin signaling mediates various biological processes such as cell proliferation, differentiation, organogenesis and tissue regeneration [6, 7]. However, constitutive activation of this signaling pathway can lead to various diseases such as osteoporosis, neurodegenerative disease, and cancer [8–10].

When the Wnt ligand binds to the LRP-5/6 receptor and the Frizzled receptor, it activates Disheveled to recruit complexes (Axin, GSK-3β, CK1, APC) to the receptor. The Wnt-Frizzled-Axin-LRP-5/6 complex then sequesters cytoplasmic GSK-3β, rendering β-catenin unphosphorylated. Free β-catenin then migrates to the nucleus, accumulates, and binds with T cell-specific factor (TCF)/lymphoid enhancer-binding factor (LEF) to regulate the expression of Wnt target genes [9, 10].

Accumulating evidence suggests that aberrant activation of Wnt/β-catenin signaling is also associated with VS tumors. Localization of β-catenin is observed in the nucleus of primary human schwannoma cells, but not Schwann cells [11]. Tissues from NF2 patients exhibit higher levels of β-catenin than normal adjacent tissues or tumors isolated from defined NF1 patients [12]. In addition, merlin encoded by the *NF2* gene can inhibit Wnt/β-catenin signaling, suggesting that Wnt/β-catenin signaling is increased in VS patients known to have NF2 loss [11–13]. It has been reported that PKF 115-584, a Wnt/β-catenin small molecule inhibitor, can inhibit the proliferation of NF2-deficient cells [13].

[1]Department of ICT Environmental Health System, Graduate School, Soonchunhyang University, Asan-si 31538, Republic of Korea; [2]Department of Biomedical Laboratory Science, College of Medical Sciences, Soonchunhyang University, Asan-si 31538, Republic of Korea; [3]Department of Otorhinolaryngology, Yonsei University, College of Medicine, Seoul 03722, Republic of Korea; [4]College of Pharmacy and Yonsei Institute of Pharmaceutical Sciences, Yonsei University, Yeonsu-gu, Incheon 21983, Republic of Korea; [5]Department of Otolaryngology-Head and Neck Surgery, Stanford University School of Medicine, Stanford, CA 94305, USA and [6]Department of Otorhinolaryngology-Head and Neck Surgery, Soonchunhyang University Bucheon Hospital, Bucheon 14584, Republic of Korea
Correspondence: Jong Dae Lee (ljdent10@gmail.com) or Sin-Aye Park (sappark@sch.ac.kr)

SPRINGER NATURE

Celastrol is a natural bioactive ingredient derived from *Tripterygium Wilfordi*, a vine plant. Recent studies of various tumor models in vitro and in vivo have shown that celastrol exhibits significant broad-spectrum anticancer activity against a variety of cancers, including gastric cancer [14, 15], breast cancer [16, 17], and glioma [18, 19]. Interestingly, some studies have reported that celastrol inhibits Wnt/β-catenin signaling. Celastrol inhibits colorectal cancer cell growth by promoting β-catenin degradation via Yes-associated protein and liver kinase B1 [20]. Celastrol also inhibits stem cell-like properties of clear cell renal cell carcinoma cells by blocking Wnt/β-catenin signaling [21]. However, studies on whether celastrol could inhibit VS tumor growth have not been reported yet. Thus, in this study, we screened a series of natural compounds that could inhibit the viability of VS cells, of which celastrol was the most effective one. Our results showed that celastrol inhibited the growth of VS cells in vitro and in vivo by inhibiting the Wnt/β-catenin signaling pathway.

MATERIALS AND METHODS

Reagents and antibodies
Celastrol (#C0869) was purchased from Sigma-Aldrich (St. Louis, MO, USA). Anti-cyclin A2 (#4656), anti-cyclin B1 (#12231), anti-cyclin D1 (#2978), anti-cyclin E2 (#4132), anti-CDK2 (#2546), anti-CDK6 (#3136), anti-β-actin (#3700), anti-caspase-3 (#14220), anti-cleaved caspase-3 (#9664), anti-PARP (#9542), anti-cleaved PARP (#5625), anti-β-catenin (#8480), anti-phopho-β-catenin (S33/S37/T41) (#9561), anti-phopho-β-catenin (S552) (#5651), anti-phopho-β-catenin (S675) (#4176), anti-c-Myc (#5605), and anti-LEF1 (#2230) were obtained from Cell Signaling Technology (Danvers, MA, USA). Anti-GSK-3β (#81462) was purchased from Santa Cruz Biotechnology (Dallas, TX, USA).

Cell line and culture
Vestibular schwannoma cell lines HEI-193 (an immortalized cell line derived from VS from human NF2 patients) and SC4 (an immortalized cell line derived from Nf2-deficient transgenic mice) were gently provided by House Ear Institute (Los Angeles, CA, USA) and cultured in DMEM (Corning Inc., Corning, NY, USA) containing 10% fetal bovine serum (FBS, Thermo Fisher Scientific, Waltham, MA, USA) and 1% penicillin/streptomycin (Corning Inc.). All cells were maintained at 37 °C in a humidified atmosphere with 5% CO_2/95% air.

High-throughput screening
For the identification of natural products that effectively inhibit the viability of VS cells, the effects of a collection of 1,019 natural products provided from the Korea Chemical Bank (KRICT, Daejeon, Republic of Korea) on cell viability were tested in HEI-193 cells. Two $\times 10^4$ HEI-193 cells were plated in 96-well microplates (Corning Inc.) and incubated for 24 h, then the cells were treated with 10 μM of the natural products for 24 h. To assess the cell viability, CellTiter 96® AQueous One Solution Cell Proliferation Assay kit (Promega, Madison, WI, USA) was used according to manufacturer's instructions. The absorbance of formazan was measured by Infinite M200 microplate reader (Tecan, Grödig, Austria) at a wavelength of 490 nm. In the primary screening, compounds that reduced cell viability by 50% or more were considered primary hits.

Human primary VS cells and sliced VS tissue preparation
All experiments based on the patients' cells and tissues were performed in accordance with the guidelines and were approved by the Severance Hospital Institutional Review Board (IRB No. 2016-2915-003). The primary VS cells were prepared from VS tumor tissues chopped with a surgical blade and digested using 0.25% Trypsin–EDTA (Thermo Fisher Scientific) for 10 min. The cells were cultured in a medium consisting of DMEM, 10% FBS, 1% penicillin/streptomycin, and 10% N2 supplement (Sigma-Aldrich). The VS tumor tissue slices were prepared from surgically removed tumors of 2-mm thickness and immersed in the medium containing DMEM, 10% FBS, 1% penicillin/streptomycin, and 10% N_2 supplement.

Cell viability assay
Cells were seeded in 96-well plates (1×10^4/well) and incubated with DMSO or celastrol for 24 h. The cells were then treated with 20 μL of CellTiter 96® Cell Proliferation Assay (Promega, #G3582) for 2 h at 37 °C. The absorbance of each well was detected at 490 nm with a Multiskan, GO microplate reader (Thermo Fisher Scientific). All procedures were performed according to the manufacturer's instructions. EdU labelling and detection was performed according to the manufacturer's instructions (Thermo Fisher Scientific, #C10337). Cells were plated on coverslips and incubated overnight. Cells were stained with EdU labeling solution for 2 h at room temperature. After fixation and permeabilization, cells were incubated with Click-iT® reaction cocktail for 30 min, followed by incubation with Hoechst® 33342 solution.

Quantitative real-time PCR
Total RNA was isolated from cells using TRIzol® (Thermo Fisher Scientific). Reverse transcription of total RNA was performed using the M-MLV reverse transcriptase (Promega). Quantitative PCR (qPCR) was performed using qPCR reagents (Enzynomics, Daejeon, Republic of Korea) and 7500 Real-Time PCR (Applied Biosystems). Primer sequences are listed in the Supplementary Table S1.

Western blot analysis
Standard sodium dodecyl sulfate-polyacrylamide gel electrophoresis (SDS-PAGE) and Western blotting were used to analyze the expression of various proteins. Cells were lysed in the lysis buffer (Cell Signaling Technology, #9803) containing protease inhibitors and phosphatase inhibitors (Roche). The quantitative protein concentration was determined by BCA Protein Assay Kit (Thermo Fisher Scientific) and equal amounts of protein were loaded on 8%-12% SDS-PAGE. Proteins were transferred to polyvinylidene difluoride membrane (Merck Millipore, Burlington, MA, USA) and subjected to immunoblotting using various antibodies overnight at 4 °C, followed by further incubation with the secondary antibody (AbFrontier, Seoul, Republic of Korea, #LF-SA8001 and LF-SA8002) at room temperature for 1 h. Visualization of protein bands was detected with Westsave Gold detection reagents (AbFrontier, #LF-QC0103).

Luciferase reporter assay
M50 Super 8 × TOPFlash and M51 Super 8×FOPFlash (TOPFlash mutant) were gifts from Randall Moon (Addgene plasmid #12456, 12457) [22]. Cells were co-transfected with these plasmids and β-galactosidase plasmid using Lipofectamine 2000 (Thermo Fisher Scientific) for 24 h and incubated with vehicle or celastrol for an additional 12 h. The luciferase and β-galactosidase enzyme activities were analyzed using the Luciferase Reporter Assay System (Promega) and β-galactosidase Enzyme Systems (Promega) according to the manufacturer's instructions.

Immunoprecipitation assay
SC4 cells were treated with vehicle or celastrol for 9 h. The cell lysates were prepared with IP Lysis Buffer (Thermo Scientific, #87787) and subjected to immunoprecipitation using anti-β-catenin antibody with conjugated protein A/G PLUS-agarose (Santa Cruz Biotechnology, #2003). Immune complexes were subjected to Western blot analysis and detected with anti-GSK-3β antibody.
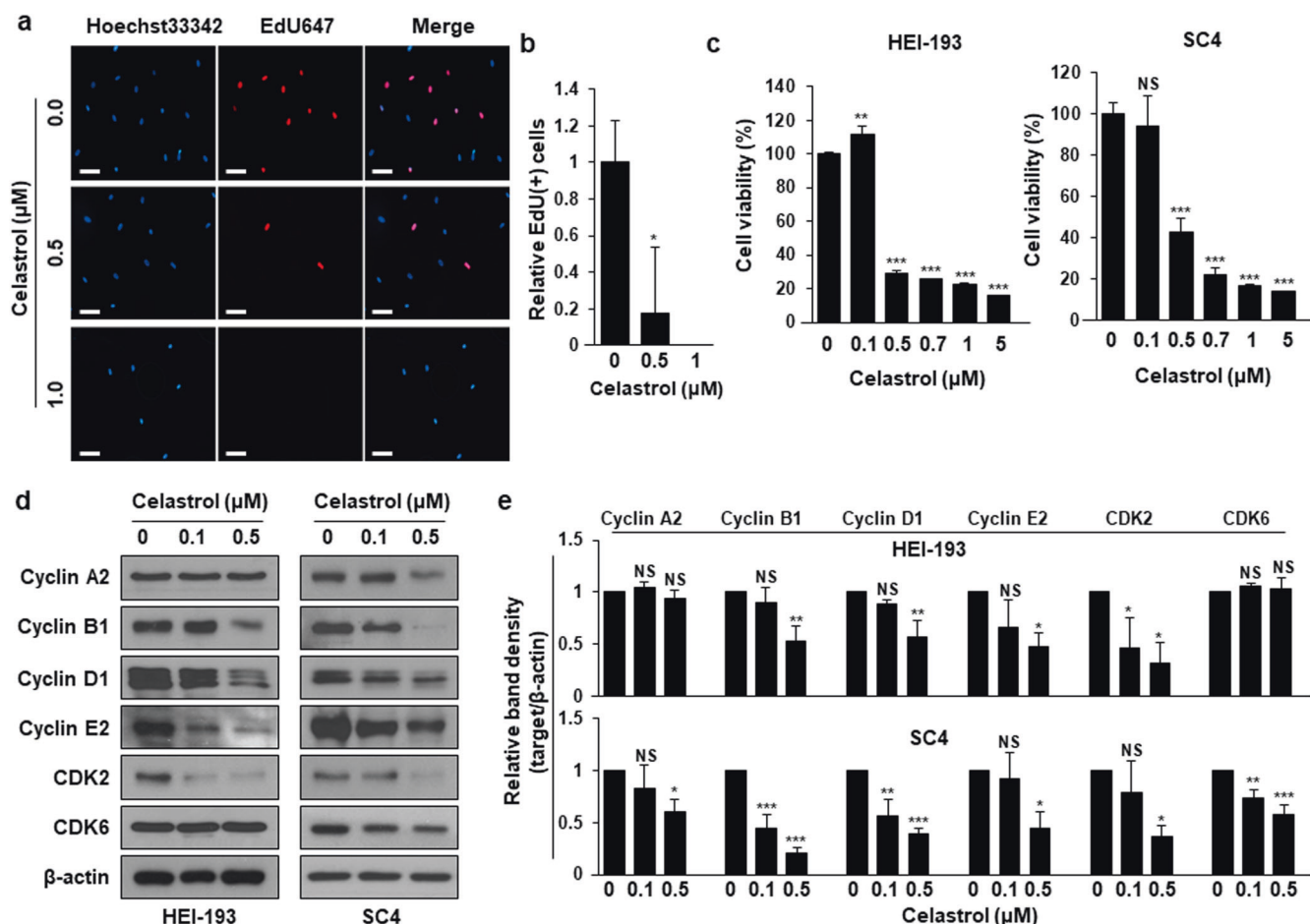
Fig. 1 Celastrol is identified as the most potent compound by HTS. a Schematic of two rounds of screening. **b** Dose-response curves quantifying cell viability after 24 h treatment of 9 candidates. SC4 cells were seeded in 96-well microplates and cultured for 24 h. The cells were treated with a series of concentrations (0.01, 0.1, 0.3, 1, 3, and 30 μM) of compounds for an additional 24 h, followed by MTS assay. **c** Structure of celastrol.

Tumor allografts in nude mice
Female BALB/c (nu/nu) athymic nude mice, 5 weeks of age (weight 17–19 g), were purchased from Orient Bio Inc. (Seongnam, Republic of Korea). Mice were maintained in specific pathogen-free conditions: 20–24 °C, 12/12 h of dark/light cycle, 60% ± 5% of humidity, and plastic cage. Bedding materials were changed every week, and environmental enrichment was done with sterile materials. For the tumor allograft assay, SC4 cells (5×10^6 cells/ HBSS 100 μL) and matrigel (BD Biosciences, NJ, USA, #354248) 100 μL were mixed well and inoculated subcutaneously into the right dorsal flank of female nude mice after isoflurane inhalation anaesthesia. When the tumors reached approximately 50–100 mm³, the tumor-bearing mice were randomly divided into two groups ($n = 4$/group). Then, vehicle and celastrol (1.25 mg/kg) were intraperitoneally administered once every 3 days for 2 weeks. At the end of the experiments, mice were euthanized by CO_2 inhalation and each tumor was removed.

Immunofluorescence staining
For staining fixed paraffin-embedded tissues, a standard protocol for deparaffinization, antigen retrieval, and permeabilisation was followed. The tissues were incubated overnight with antibodies at 4 °C, washed with PBS, and incubated further with Alexa Fluor 488 antibody (Thermo Fisher Scientific) for 1 h at room temperature. After washing, the tissues were stained using ProLong® Gold Antifade Reagent containing DAPI (Thermo Fisher Scientific).

Statistical analysis
Data were expressed as the mean ± SD of results obtained from at least three independent experiments. Significant differences were determined by a Student's t-test or one-way ANOVA. A P-value of less than 0.05 was considered to be statistically significant.

Ethical statement
All animal experiments were performed in accordance with the guidelines for animal treatment of Soonchunhyang University. All experimental protocols in our study were conducted on protocols approved by the Institutional Animal Care and Use Committee of the Soonchunhyang University (SCH21-0010).

RESULTS
Celastrol is one of the hit compounds discovered through high-throughput screening using VS cells
To investigate potent natural compounds with cell growth inhibitory effects on VS, high-throughput screening (HTS) was performed using HEI-193 cells, an immortalized cell line derived from VS from human NF2 patients. A compound library containing 1019 natural compounds was screened at a final concentration of 10 μM. Cell viability was determined using MTS assay at 24 h after compound treatment. The primary screening of HTS revealed 44 compounds that reduced cell viabilities by more than 50%, of which 11 were ineffective at 5 μM. Thus, the remaining 33 compounds were considered as primary candidates (Fig. 1a).

Fig. 2 Celastrol inhibits the growth of VS cells. a Primary human VS cells were treated with celastrol for 24 h. Cell proliferation was analyzed by EdU staining assay. Scale bar = 100 μm. **b** Relative EdU positive cells were quantified. **c** HEI-193 and SC4 cells were treated with various concentrations of celastrol for 24 h, followed by cell proliferation assay. **d** HEI-193 and SC4 cells were incubated with celastrol for 18 h, and lysates were analyzed for the expression of indicated proteins by Western blot analysis. **e** Bar graphs indicate the relative band density in Western blot analysis. All data are presented using triplicate wells per group or three independent blots and statistical significance was determined by one-way ANOVA. *, $P < 0.05$; **, $P < 0.01$; ***, $P < 0.001$; NS, not significant.

Because SC4 cells derived from Nf2-deficient transgenic mice exhibited more aggressive growth behavior than HEI-193 cells, in the secondary screening, $Nf2^{-/-}$ SC4 cells were treated with 33 compounds for 24 h and then the final nine candidates have been selected (Fig. 1a). As shown in Fig. 1b, SC4 cells were treated with 0.01, 0.1, 0.3, 1, 3, and 30 μM of nine candidates for 24 h, and all had IC$_{50}$ values of 0 to 3 μM based on cell viabilities of SC4 cells. Celastrol (Fig. 1c) had the most potent inhibitory effect on the viability of VS cells, with an IC$_{50}$ value of 0.5 μM.

Celastrol inhibits the proliferation of VS cells
To evaluate the effect of celastrol on cell viability, primary human VS cells were treated with celastrol (0.5 and 1 μM) for 24 h and then analyzed after EdU staining. Celastrol significantly inhibited the viability of primary human VS cells in a dose-dependent manner (Fig. 2a, b). To confirm the effect of celastrol on HEI-193 and SC4 cells that were primarily screened through HTS, these cell lines were treated with celastrol for 24 h and then analyzed using the CellTiter 96® cell proliferation assay kit. The proliferation of both cell lines was significantly inhibited by celastrol at 0.5 μM (Fig. 2c). However, under the same conditions, celastrol 0.5 μM had little effect on the viability of normal Schwann cells RSC96 and HSC. Our results showed that the IC$_{50}$ value of celastrol was 0.5 μM in SC4 cells, 2.3 μM in RSC96, and 4.47 μM in HSC. The selectivity

index was calculated by comparing the celastrol IC$_{50}$ values of RSC96 or HSC cell lines with those of SC4 cells, and the values were 4.6 and 8.94, respectively (Supplementary Fig. S1). Consistent with the above results, expression levels of cell cycle-related proteins including cyclin B1, cyclin D1, cyclin E2, and CDK2 were significantly reduced by celastrol treatment (Fig. 2d, e). Also, celastrol induced cell cycle arrest at the G$_0$–G$_1$ phase, which was accompanied by a decrease in the S phase and a significant decrease in the G$_2$/M phase in SC4 cells (Supplementary Fig. S2). Collectively, these results indicate that celastrol can suppress the viability and proliferation of VS cells.

Celastrol induces apoptosis of VS cells
To further investigate the effect of celastrol on VS cell death, we utilized an apoptosis/necrosis assay kit to reveal cell apoptosis (green), necrosis (green and/or red), and healthy cells (blue) by fluorescence microscopy. SC4 cells were treated with 0.1 or 0.5 μM of celastrol for 9 h followed by analysis. As shown in Fig. 3a, b, apoptosis was significantly increased by treatment with 0.5 μM celastrol. In agreement with the above findings, levels of cleaved caspase-3 and cleaved PARP were significantly increased in HEI-193 and SC4 cells by treatment with 0.5 μM celastrol (Fig. 3c, d). These results indicate that celastrol can induce apoptosis of VS cells.
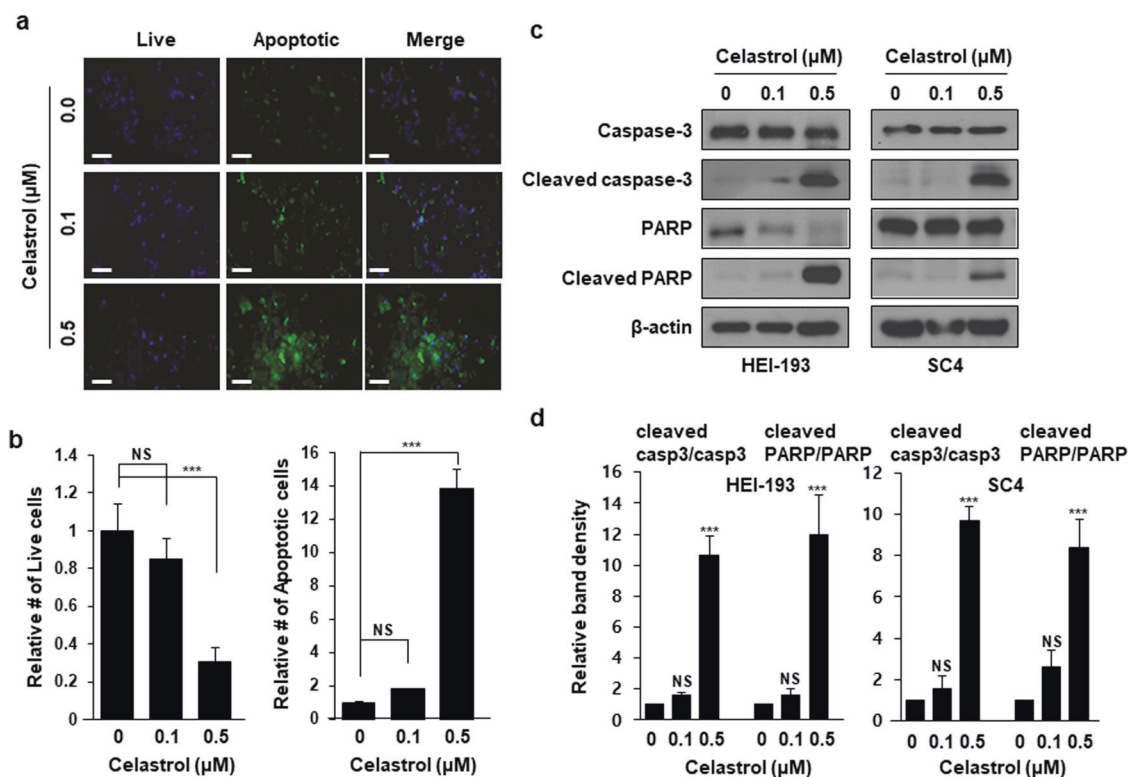
Fig. 3 Celastrol induces apoptosis of VS cells. a HEI-193 and SC4 cells were treated with celastrol for 9 h, and apoptotic or necrotic cells were determined by apoptosis/necrosis assay. Apoptosis (green), necrosis (green and/or red) and healthy cells (blue) were analyzed by fluorescence microscopy. Scale bar = 200 μm. **b** Relative number of live or apoptotic cells were quantified. **c** HEI-193 and SC4 cells were treated with celastrol for 18 h, and lysates were analyzed for the expression of indicated proteins. **d** Bar graphs indicate the relative band density in Western blot analysis. All data are presented using triplicate wells or three independent blots per group and statistical significance was determined by one-way ANOVA. ***, $P < 0.001$; NS, not significant.

Celastrol decreases Wnt/β-catenin signaling

Aberrant activation of Wnt/β-catenin signaling has been observed in primary human schwannoma cells [11] and schwannomas isolated from clinically defined NF2 patients compared to normal adjacent tissues or tumors isolated from defined NF1 patients [12]. We evaluated whether celastrol could inhibit the transcriptional activation of TCF/LEF known to regulate Wnt/β-catenin target genes. Results of β-catenin/TCF-dependent luciferase reporter (Top-luc) assay showed that celastrol reduced TOPFlash reporter activity in HEI-193 and SC4 cells. In contrast, the activity of FOPFlash (a negative control reporter with mutated β-catenin/TCF binding sites) was not affected by celastrol treatment (Fig. 4a). In addition, expression levels of β-catenin and its target proteins c-Myc and LEF1 were reduced by celastrol treatment (Fig. 4b, c). Celastrol treatment resulted in a decrease in β-catenin, especially in the nuclear fraction of SC4 cells (Supplementary Fig. S3). The inhibitory effect of celastrol on the expression of β-catenin and c-Myc in VS cells was also confirmed by immunofluorescence staining (Fig. 4d). However, mRNA levels of β-catenin were not inhibited by treatment with 0.5 μM celastrol, although it affected its protein expression levels (Fig. 4e). These results suggest that celastrol can inhibit Wnt/β-catenin signaling by suppressing the protein level, but not the mRNA level, of β-catenin.

Celastrol accelerates proteosomal degradation of β-catenin

To further determine whether celastrol could promote the degradation of β-catenin, HEI-193 and SC4 cells were treated with celastrol in the presence of CHX, an inhibitor of *de novo* protein synthesis. As shown in Fig. 5a, b, the degradation of β-catenin was accelerated after 24 h treatment with celastrol.

Since the expression of β-catenin in the cytoplasm is regulated by proteasome-mediated degradation, we next investigated whether the proteasome was involved in the degradation of β-catenin by celastrol. Although celastrol inhibited the protein level of β-catenin, this effect was diminished by treatment with MG132, a proteasome inhibitor, indicating that celastrol promoted the degradation of β-catenin via the proteasome pathway (Fig. 5c, d).

The degradation of β-catenin by the proteasome requires processes such as destructive complex formation and phosphorylation of β-catenin. As shown in Fig. 5e, celastrol enhanced the binding of β-catenin to GSK-3β, one of major destruction components. Additionally, celastrol enhanced the phosphorylation of Ser33/37/Thr41 of β-catenin but decreased the phosphorylation of Ser552 and Ser675, suggesting that it increased β-catenin degradation (Fig. 5f, g). These results demonstrated that celastrol increased the formation of the β-catenin destruction complex, which increased the phosphorylation and degradation of β-catenin.

Celastrol inhibits the growth of allograft tumors

To determine whether celastrol could suppress tumor growth in vivo, SC4 cells were subcutaneously injected into right flanks of nude mice. After the tumor volume reached approximately 50–100 mm³, mice were randomly divided into two groups ($n = 4$/group). Initially, tumor-bearing mice were treated intraperitoneally with 1.25 mg·kg^{-1}·d^{-1} or 10 mg·kg^{-1}·d^{-1} of celastrol. However, the group dosed with 10 mg kg^{-1}·d^{-1} showed a significant body weight loss and this dose was judged to be toxic. Thus, subsequent animal studies were performed only at a low dose of 1.25 mg·kg^{-1}·d^{-1}. Mice treated with celastrol once every
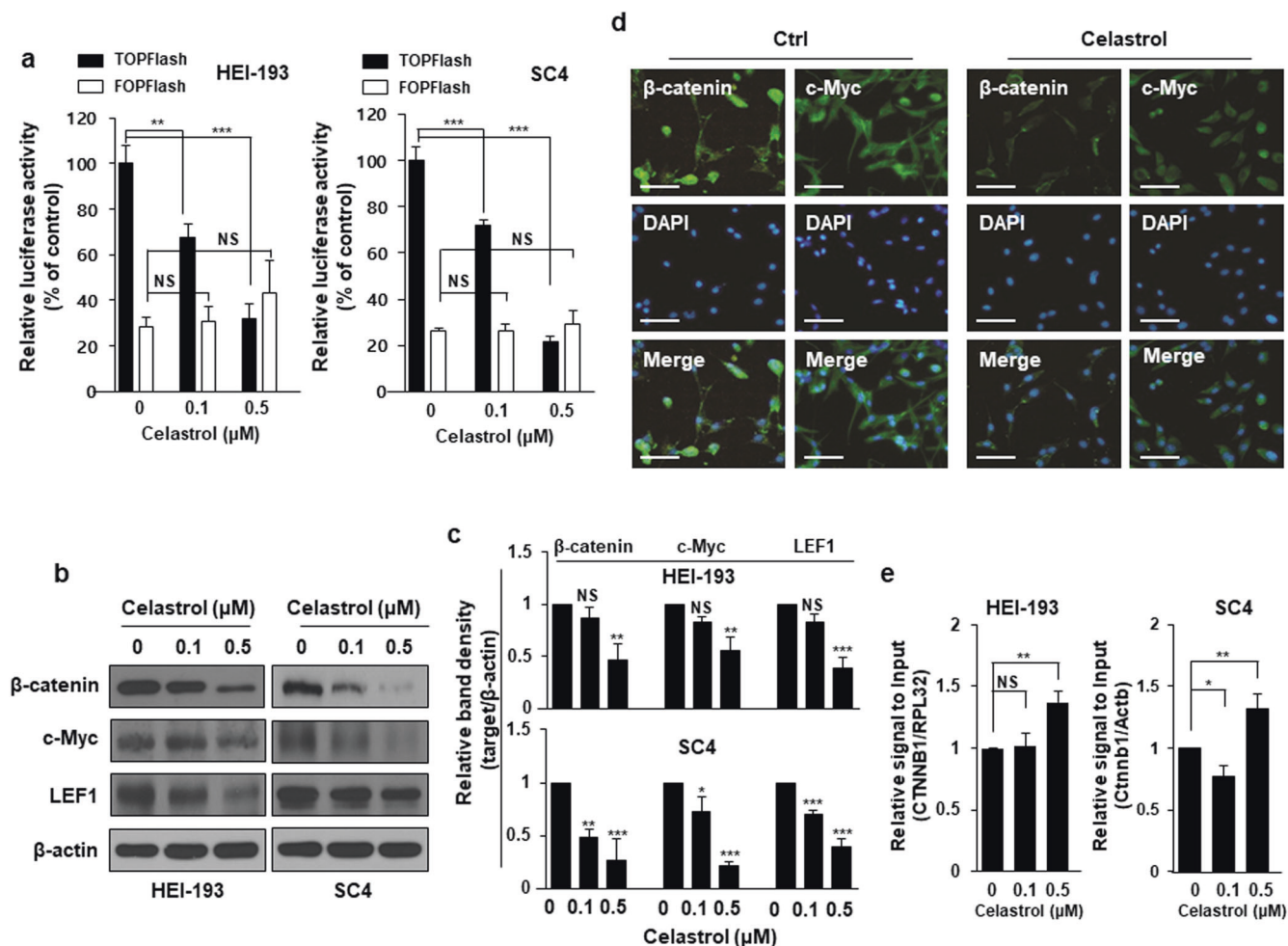
Fig. 4 Celastrol inhibits the Wnt/β-catenin signaling in VS cells. a HEI-193 and SC4 cells were transfected with TOPFlash or FOPFlash luciferase reporter plasmid for 24 h. Cells were treated with celastrol for an additional 12 h, and the luciferase activity was measured. **b** HEI-193 and SC4 cells were treated with celastrol for 18 h, and lysates were analyzed for the expression of indicated proteins. **c** Bar graphs indicate the relative band density in Western blot analysis. **d** Cells were treated with 0.5 μM celastrol for 18 h, and the intracellular expressions of β-catenin and c-Myc were analyzed by immunofluorescence staining. Scale bar = 200 μm. **e** Cells were treated with celastrol for 18 h, and the mRNA level of CTNNB1 (β-catenin) was quantitated by qPCR analysis. All data are presented using triplicate wells or three independent blots per group and statistical significance was determined by one-way ANOVA. *, $P < 0.05$; **, $P < 0.01$; ***, $P < 0.001$; NS, not significant.

3 days for 2 weeks showed significantly suppressed tumor growth compared to vehicle-treated mice (Fig. 6a-c). To further confirm effects of celastrol in vivo, levels of β-catenin, cyclin D1, and c-myc were analyzed by immunofluorescence staining. As shown in Fig. 6d, expression levels of indicated proteins were reduced in celastrol-treated tumor tissues.

There were no significant differences in body weight between vehicle- or celastrol-treated mice (Supplementary Fig. S4a). Celastrol-treated mice did not show any obvious toxicity in liver, spleen, or kidney tissues (Supplementary Fig. S4b). There was no significant difference in ALT, AST, BUN, or creatinine level between vehicle- and celastrol-treated mice (Supplementary Fig. S4c). Taken together, these results demonstrate that celastrol can inhibit tumor growth of VS in vivo.

DISCUSSION
Several clinical trials for NF2 including VS are ongoing [23, 24]. However, most of these trials rely on expensive chemotherapeutic agents with serious side effects, including cardiovascular toxicity [25]. Although many studies have been conducted on effects of existing anticancer drugs that inhibit molecular targets such as VEGF, EGFR/ErbB2, PDGF, PI3K/AKT, PAK, and mTORC1 [24], these molecular targets are not specific to NF2 therapy. Therefore, there is a need for the development of drugs targeting molecular markers critically involved in VS tumor development.

The pathogenesis of VS is associated with a genetic defect in the tumor suppressor gene merlin. It has been reported that when merlin defect occurs, Wnt/β-catenin activation proceeds and tumors occur [11, 26]. Loss of merlin gene increases nuclear transcriptional activity of β-catenin in a Rac protein-dependent manner [13]. As merlin inhibits FOXM1 protein, destabilizing FOXM1/β-catenin and loss of Merlin might increase nuclear β-catenin transcriptional activity by inducing stabilization of FOXM1 protein [27]. In addition, merlin inhibits Wnt/β-catenin signaling by blocking LRP6 phosphorylation, which is required for Wnt signaling [12]. Therefore, loss of merlin can induce sustained phosphorylation of LRP and increase the activity of Wnt/β-catenin signaling. These studies suggest that Wnt/β-catenin signaling might be an important molecular target in drug development for VS.

Numerous clinical trial studies have been conducted to develop therapeutics targeting the Wnt pathway in various
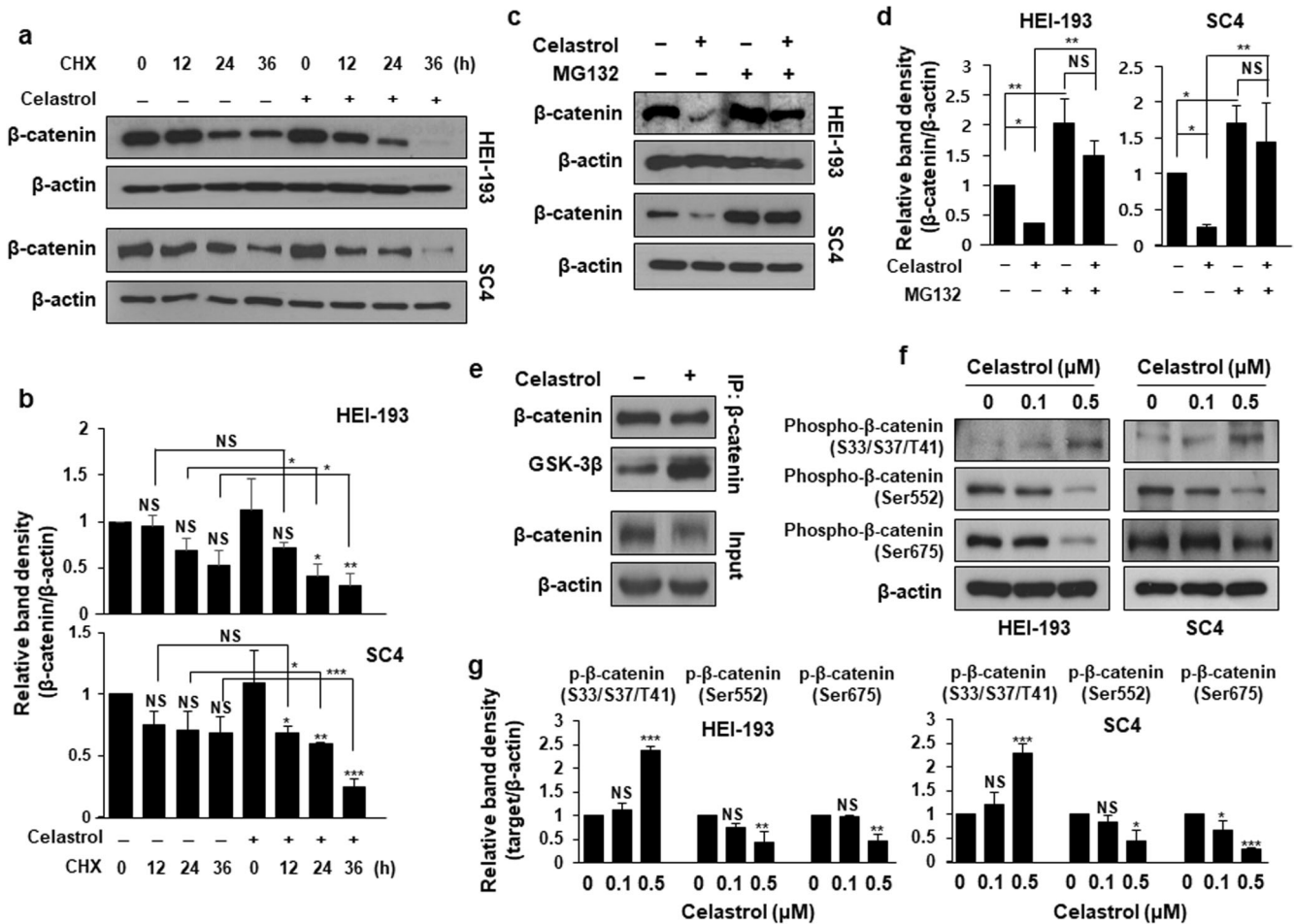
Fig. 5 **Celastrol promotes the degradation of β-catenin in VS cells. a** HEI-193 and SC4 cells were treated with CHX (50 μg/mL) in the presence of DMSO or celastrol (0.5 μM) for the indicated time intervals. The cell lysates were analyzed for the expression of β-catenin. **c** Cells were treated with 0.5 μM celastrol for 10 h, then incubated with or without MG132 (10 μM) for an additional 8 h. The cell lysates were subjected to Western blotting to determine the expression of β-catenin. **e** Lysates from SC4 cells after treatment with vehicle or celastrol (0.5 μM) were immunoprecipitated with β-catenin antibody. The immunoprecipitated fractions were analyzed by immunoblotting with the indicated antibodies. **f** Cells were treated with celastrol for 18 h, and lysates were analyzed for the expression of indicated proteins. **b, d, g** Bar graphs indicate the relative band density in Western blot analysis. Data are presented using three independent blots per group and statistical significance was determined by one-way ANOVA. *, $P < 0.05$; **, $P < 0.01$; ***, $P < 0.001$; NS, not significant.

carcinomas [8, 28]. However, it is still difficult to develop therapeutic agents targeting Wnt, an important regulatory factor for embryonic development and maintenance of tissue homeostasis [8]. WNT974 is an inhibitor of Porcupine, an O-acyltransferase that mediates the secretion of Wnt ligand. It has side effects such as decreased bone mass and decreased muscle strength [29]. OMP-18R5 (Vantictumab) and OMP-54F28 (Ipafricept) can inhibit Wnt/β-catenin signaling by blocking the binding of Wnt ligand to FZD. However, they also have side effects such as vomiting, abdominal pain, and bone metabolic disease [30]. Since these drugs have too severe side effects to treat VS, a non-malignant tumor, effective drugs with minimal side effects need to be developed for the treatment of VS.

Dietary products found in fruits and vegetables can inhibit several cellular signaling pathways important in the pathogenesis of cancer. Some of these products can be used to treat and prevent cancer [31–33]. Celastrol is one of the most potent naturally-derived chemotherapeutic agents effective against a variety of cancers [34]. Unfortunately, celastrol has poor physicochemical properties, which may cause difficulties in formulation development. It has also been found to be toxic to the heart [35, 36], liver [37, 38] and hematopoietic system [39].

However, structural modifications of celastrol can improve its biological activities such as stability and solubility [34]. Various types of nano/microcarriers such as liposomes [40], polymer micelles [41], and nanoparticles [42, 43] have been studied to improve the efficacy of celastrol. In addition, combination of celastrol with chemotherapeutic agents [44, 45], the tumor necrosis factor superfamily [46, 47], and ionizing radiation [48, 49] can successfully improve its therapeutic efficacy and lower the toxicity of celastrol.

Because VS is a benign, non-metastatic tumor, delaying tumor growth can improve the quality of life and prolong the life expectancy of patients. Therefore, it is necessary to discover a Wnt/β-catenin targeting therapeutic candidate that VS patients can take for life with a low toxicity. Our results demonstrated that celastrol effectively inhibited the growth of VS cells at a low concentration both in vitro and in vivo. In particular, we demonstrate for the first time that celastrol targets Wnt/β-catenin signaling important for VS tumor development and promotes the degradation of β-catenin. Although there are still challenges in the development of celastrol as a treatment for VS, our results suggest that celastrol is a potential therapeutic agent for treating VS.
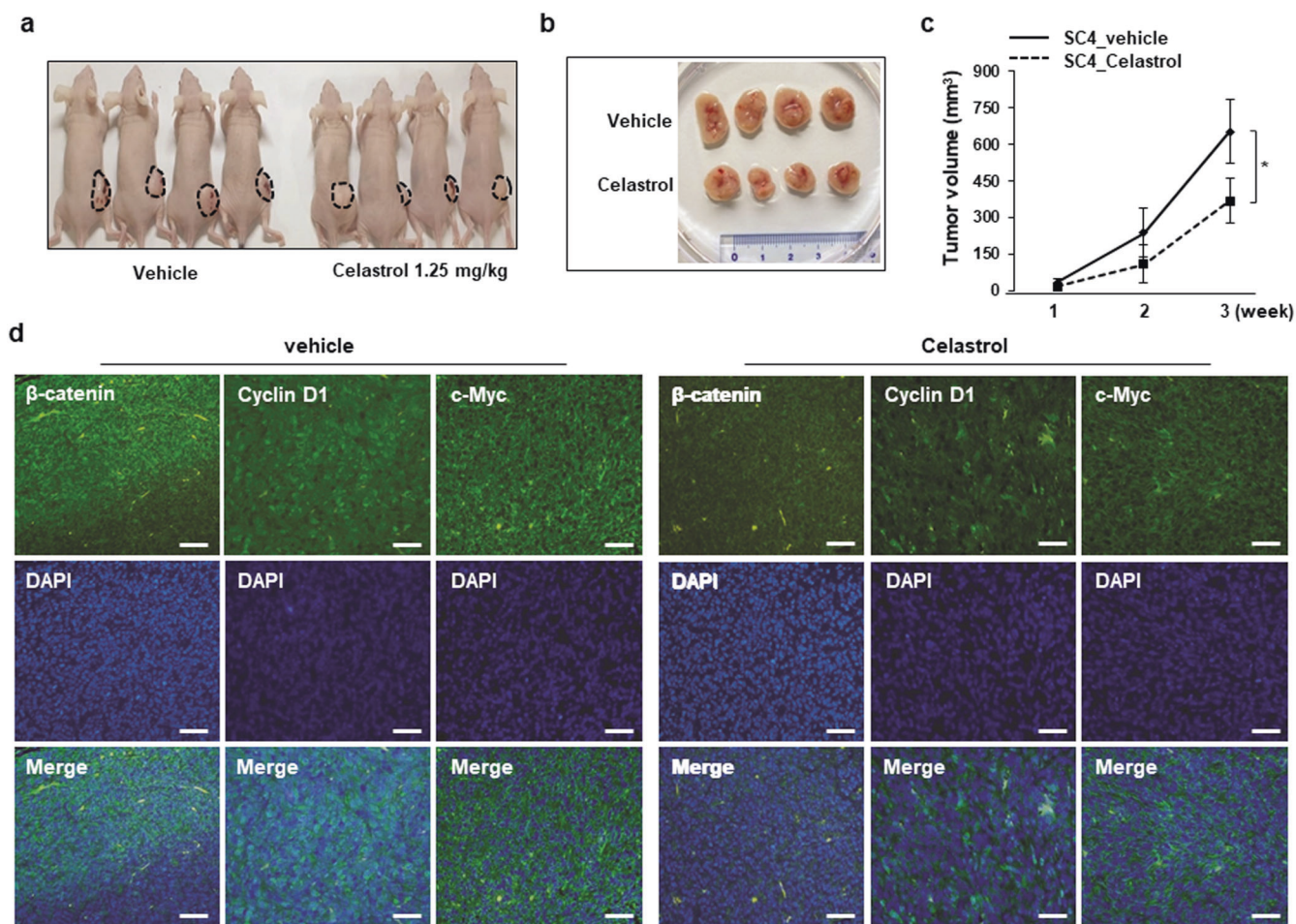
Fig. 6 Celastrol suppresses the tumor growth of VS in vivo. Images of SC4 tumor-bearing mice (**a**) and tumors (**b**) after vehicle or celastrol treatment. SC4 cells were subcutaneously injected into BALB/c nude mice. Intraperitoneal treatment with vehicle or celestrol was administered once every 3 days for 2 weeks. **c** Tumor volume was monitored for 3 weeks. **d** Representative immunofluorescence images of β-catenin, cyclin D1, and c-Myc in tumors after vehicle or celastrol treatment. Scale bar = 50 μm. Two-sided t test. *, $P < 0.05$.

AUTHOR CONTRIBUTIONS
JDL and SAP conceived and designed the experiments; NHK, MK, JJ, HBC, and JL performed the experiments; NHK, YJY, ISM, HKL, WN, KMS, and SAL analyzed the data; JDL and SAP wrote the manuscript.

ADDITIONAL INFORMATION
Supplementary information The online version contains supplementary material available at https://doi.org/10.1038/s41401-022-00908-4.

Competing interests: The authors declare no competing interests.

REFERENCES
1. Evans DG. Neurofibromatosis 2 [bilateral acoustic neurofibromatosis, central neurofibromatosis, NF2, neurofibromatosis type II]. Genet Med. 2009;11:599–610.
2. Petrilli AM, Fernandez-Valle C. Role of merlin/NF2 inactivation in tumor biology. Oncogene. 2016;35:537–48.
3. Evans DG. Neurofibromatosis type 2 (NF2): a clinical and molecular review. Orphanet J Rare Dis. 2009;4:16.
4. Goldbrunner R, Weller M, Regis J, Lund-Johansen M, Stavrinou P, Reuss D, et al. EANO guideline on the diagnosis and treatment of vestibular schwannoma. Neuro Oncol. 2020;22:31–45.
5. Plans G, Torres A, Ferran E, Aparicio A, Acebes JJ. Contralateral hearing loss after vestibular schwannoma surgery: case report. Neurosurgery. 2007;61:E878. discussion E878.
6. Clevers H. Wnt/beta-catenin signaling in development and disease. Cell. 2006; 127:469–80.
7. Nejak-Bowen K, Monga SP. Wnt/beta-catenin signaling in hepatic organogenesis. Organogenesis. 2008;4:92–9.
8. Jung YS, Park JI. Wnt signaling in cancer: therapeutic targeting of Wnt signaling beyond beta-catenin and the destruction complex. Exp Mol Med. 2020;52:183–91.
9. Krishnamurthy N, Kurzrock R. Targeting the Wnt/beta-catenin pathway in cancer: update on effectors and inhibitors. Cancer Treat Rev. 2018;62:50–60.
10. Zhan T, Rindtorff N, Boutros M. Wnt signaling in cancer. Oncogene. 2017;36: 1461–73.
11. Zhou L, Ercolano E, Ammoun S, Schmid MC, Barczyk MA, Hanemann CO. Merlin-deficient human tumors show loss of contact inhibition and activation of Wnt/beta-catenin signaling linked to the PDGFR/Src and Rac/PAK pathways. Neoplasia. 2011;13:1101–12.
12. Kim M, Kim S, Lee SH, Kim W, Sohn MJ, Kim HS, et al. Merlin inhibits Wnt/beta-catenin signaling by blocking LRP6 phosphorylation. Cell Death Differ. 2016;23: 1638–47.
13. Bosco EE, Nakai Y, Hennigan RF, Ratner N, Zheng Y. NF2-deficient cells depend on the Rac1-canonical Wnt signaling pathway to promote the loss of contact inhibition of proliferation. Oncogene. 2010;29:2540–9.
14. Lee HW, Jang KS, Choi HJ, Jo A, Cheong JH, Chun KH. Celastrol inhibits gastric cancer growth by induction of apoptosis and autophagy. BMB Rep. 2014;47: 697–702.

15. Sha M, Ye J, Zhang LX, Luan ZY, Chen YB, Huang JX. Celastrol induces apoptosis of gastric cancer cells by miR-21 inhibiting PI3K/Akt-NF-kappaB signaling pathway. Pharmacology. 2014;93:39–46.

16. Kim Y, Kang H, Jang SW, Ko J. Celastrol inhibits breast cancer cell invasion via suppression of NF-kB-mediated matrix metalloproteinase-9 expression. Cell Physiol Biochem. 2011;28:175–84.

17. Mi C, Shi H, Ma J, Han LZ, Lee JJ, Jin X. Celastrol induces the apoptosis of breast cancer cells and inhibits their invasion via downregulation of MMP-9. Oncol Rep. 2014;32:2527–32.

18. Huang Y, Zhou Y, Fan Y, Zhou D. Celastrol inhibits the growth of human glioma xenografts in nude mice through suppressing VEGFR expression. Cancer Lett. 2008;264:101–6.

19. Liu X, Zhao P, Wang X, Wang L, Zhu Y, Song Y, et al. Celastrol mediates autophagy and apoptosis via the ROS/JNK and Akt/mTOR signaling pathways in glioma cells. J Exp Clin Cancer Res. 2019;38:184.

20. Wang S, Ma K, Zhou C, Wang Y, Hu G, Chen L, et al. LKB1 and YAP phosphorylation play important roles in celastrol-induced beta-catenin degradation in colorectal cancer. Ther Adv Med Oncol. 2019;11:1758835919843736.

21. Zhang CJ, Zhu N, Wang YX, Liu LP, Zhao TJ, Wu HT, et al. Celastrol attenuates lipid accumulation and stemness of clear cell renal cell carcinoma via CAV-1/LOX-1 pathway. Front Pharmacol. 2021;12:658092.

22. Veeman MT, Slusarski DC, Kaykas A, Louie SH, Moon RT. Zebrafish prickle, a modulator of noncanonical Wnt/Fz signaling, regulates gastrulation movements. Curr Biol. 2003;13:680–5.

23. Fujii M, Kobayakawa M, Saito K, Inano A, Morita A, Hasegawa M, et al. Rationale and design of BeatNF2 trial: a clinical trial to assess the efficacy and safety of Bevacizumab in patients with neurofibromatosis type 2 related vestibular schwannoma. Curr Oncol. 2021;28:726–39.

24. Long J, Zhang Y, Huang X, Ren J, Zhong P, Wang B. A review of drug therapy in vestibular schwannoma. Drug Des Dev Ther. 2021;15:75–85.

25. Florescu M, Cinteza M, Vinereanu D. Chemotherapy-induced cardiotoxicity. Maedica. 2013;8:59–67.

26. Mota M, Shevde LA. Merlin regulates signaling events at the nexus of development and cancer. Cell Commun Signal. 2020;18:63.

27. Quan M, Cui J, Xia T, Jia Z, Xie D, Wei D, et al. Merlin/NF2 suppresses pancreatic tumor growth and metastasis by attenuating the FOXM1-mediated Wnt/beta-catenin signaling. Cancer Res. 2015;75:4778–89.

28. Harb J, Lin PJ, Hao J. Recent development of Wnt signaling pathway inhibitors for cancer therapeutics. Curr Oncol Rep. 2019;21:12.

29. Madan B, McDonald MJ, Foxa GE, Diegel CR, Williams BO, Virshup DM. Bone loss from Wnt inhibition mitigated by concurrent alendronate therapy. Bone Res. 2018;6:17.

30. Jimeno A, Gordon M, Chugh R, Messersmith W, Mendelson D, Dupont J, et al. A first-in-human phase I study of the anticancer stem cell agent Ipafricept (OMP-54F28), a decoy receptor for Wnt ligands, in patients with advanced solid tumors. Clin Cancer Res. 2017;23:7490–7.

31. Li Y, Li S, Meng X, Gan RY, Zhang JJ, Li HB. Dietary natural products for prevention and treatment of breast cancer. Nutrients. 2017;9:728.

32. Mann J. Natural products in cancer chemotherapy: past, present and future. Nat Rev Cancer. 2002;2:143–8.

33. Reddy L, Odhav B, Bhoola KD. Natural products for cancer prevention: a global perspective. Pharmacol Ther. 2003;99:1–13.

34. Shi J, Li J, Xu Z, Chen L, Luo R, Zhang C, et al. Celastrol: a review of useful strategies overcoming its limitation in anticancer application. Front Pharmacol. 2020;11:558741.

35. Sun H, Liu X, Xiong Q, Shikano S, Li M. Chronic inhibition of cardiac Kir2.1 and HERG potassium channels by celastrol with dual effects on both ion conductivity and protein trafficking. J Biol Chem. 2006;281:5877–84.

36. Liu C, Zhang C, Wang W, Yuan F, He T, Chen Y, et al. Integrated metabolomics and network toxicology to reveal molecular mechanism of celastrol induced cardiotoxicity. Toxicol Appl Pharmacol. 2019;383:114785.

37. Jin C, Wu Z, Wang L, Kanai Y, He X. CYP450s-activity relations of celastrol to interact with Triptolide reveal the reasons of hepatotoxicity of Tripterygium wilfordii. Molecules. 2019;24:2162.

38. Sun M, Tang Y, Ding T, Liu M, Wang X. Inhibitory effects of celastrol on rat liver cytochrome P450 1A2, 2C11, 2D6, 2E1 and 3A2 activity. Fitoterapia. 2014;92:1–8.

39. Kusy S, Ghosn EE, Herzenberg LA, Contag CH. Development of B cells and erythrocytes is specifically impaired by the drug celastrol in mice. PLoS One. 2012;7:e35733.

40. Song J, Shi F, Zhang Z, Zhu F, Xue J, Tan X, et al. Formulation and evaluation of celastrol-loaded liposomes. Molecules. 2011;16:7880–92.

41. Zhao Y, Tan Y, Meng T, Liu X, Zhu Y, Hong Y, et al. Simultaneous targeting therapy for lung metastasis and breast tumor by blocking the NF-kappaB signaling pathway using celastrol-loaded micelles. Drug Deliv. 2018;25:341–52.

42. Chen Y, Zhou L, Yuan L, Zhang ZH, Liu X, Wu Q. Formulation, characterization, and evaluation of in vitro skin permeation and in vivo pharmacodynamics of surface-charged tripterine-loaded nanostructured lipid carriers. Int J Nanomed. 2012;7:3023–32.

43. Sanna V, Chamcheu JC, Pala N, Mukhtar H, Sechi M, Siddiqui IA. Nanoencapsulation of natural triterpenoid celastrol for prostate cancer treatment. Int J Nanomed. 2015;10:6835–46.

44. Raja SM, Clubb RJ, Ortega-Cava C, Williams SH, Bailey TA, Duan L, et al. Anticancer activity of celastrol in combination with ErbB2-targeted therapeutics for treatment of ErbB2-overexpressing breast cancers. Cancer Biol Ther. 2011;11:263–76.

45. Shanmugam MK, Ahn KS, Lee JH, Kannaiyan R, Mustafa N, Manu KA, et al. Celastrol attenuates the invasion and migration and augments the anticancer effects of Bortezomib in a xenograft mouse model of multiple myeloma. Front Pharmacol. 2018;9:365.

46. Nazim UM, Yin H, Park SY. Autophagy flux inhibition mediated by celastrol sensitized lung cancer cells to TRAIL-induced apoptosis via regulation of mitochondrial transmembrane potential and reactive oxygen species. Mol Med Rep. 2019;19:984–93.

47. Cha Z, Cheng J, Xiang H, Qin J, He Y, Peng Z, et al. Celastrol enhances TRAIL-induced apoptosis in human glioblastoma via the death receptor pathway. Cancer Chemother Pharmacol. 2019;84:719–28.

48. Lee JH, Choi KJ, Seo WD, Jang SY, Kim M, Lee BW, et al. Enhancement of radiation sensitivity in lung cancer cells by celastrol is mediated by inhibition of Hsp90. Int J Mol Med. 2011;27:441–6.

49. Jun HY, Kim TH, Choi JW, Lee YH, Lee KK, Yoon KH. Evaluation of connectivity map-discovered celastrol as a radiosensitizing agent in a murine lung carcinoma model: feasibility study of diffusion-weighted magnetic resonance imaging. PLoS One. 2017;12:e0178204.